Chemistry of Heterocyclic Compounds, Vol. 46, No. 3, 2010

PHOTOCHROMIC AND THERMOCHROMIC SPIRANES 33.* SYNTHESIS OF A NEW INDOLINONAPHTHOXAZINO-BISSPIROPYRAN AND INVESTIGATION OF ITS PHOTOCHROMIC CHARACTERISTICS**

E. L. Mukhanov[1], Yu. S. Alekseenko[2], I. V. Dorogan[1], V. V. Tkachev[3], B. S. Lukyanov[1]*, S. M. Aldoshin[3], S. O. Bezuglyi[2], V. I. Minkin[1], A. N. Utenyshev[3], and O. N. Ryashchin[1]**

*A new unsymmetrical bisspiropyran was synthesized on the basis of 2,4-dihydroxyisophthalic aldehyde with naphthoxazinone and indoline fragments in the structure. The structure of the obtained compound was proved by the data from ^{1}H NMR and IR spectroscopy and X-ray crystallographic analysis. The photochromic characteristics of the obtained compound were investigated. It was established by means of the data from B3LYP/6-31G** quantum-chemical calculations that irradiation of a solution of the obtained biphotochrome with unfiltered light leads to opening of both pyran fragments. This is the first corroborated example of the twofold cleavage of C_{spiro}–O bonds for compounds of this class.*

Keywords: bisspiropyran, merocyanine, TD DFT, photochromism.

Spiropyrans and their related compounds are widely known classes of organic photochromes [2]. The possibility of controlled variation of the photochromic characteristics of the compounds with wide variation of the structure is an important factor that arouses the interest of researchers in these subjects [3, 4]. Special attention has been drawn to the bisspiropyrans **1** – structures with two bisspiropyran fragments combined in one molecule.

---

*For Communication 32 see [1].

** Dedicated to Professor M. A. Yurovskaya on her birthday.

*** To whom correspondence should be addressed, e-mail: bluk@ipoc.rsu.ru.

[1]Research Institute of Physical and Organic Chemistry, Southern Federal University, Rostov-on-Don 344090, Russia.

[2]Southern Scientific Center, Russian Academy of Sciences, Rostov-on-Don 344090, Russia.

[3]Institute of Problems of Chemical Physics, Russian Academy of Sciences, Chernogolovka 142432, Moscow Region, Russia.

Translated from Khimiya Geterotsiklicheskikh Soedinenii, No. 3, pp. 357-372, March, 2010. Original article submitted February 2, 2010.

The presence of two photochromic centers with potentially nonequivalent photoisomerization parameters and spectral characteristics of the photoinduced merocyanine forms makes such compounds prospective components of molecular switches. The possible strong bathochromic shift of the maximum of the doubly opened bisspiropyran makes it possible to use them for the creation of data carriers that can be overwritten by suitable mid-IR radiation [5].

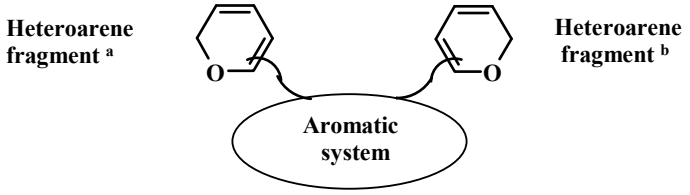

1

On the basis of 8'-formyl 7'-hydroxy-3-methyl-4-oxospiro(2,3-dihydronaphtho[2,1-*e*][1,3]oxazine-2,2'-[3H]-chromene) (**2**) we obtained the new unsymmetrical bisspiropyran **3** [6].

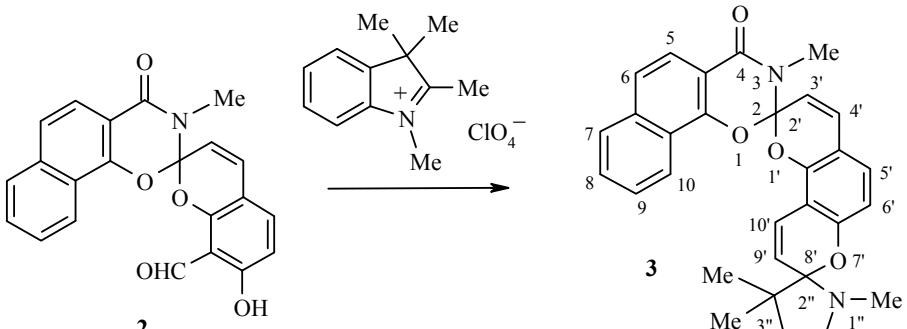

2 **3**

For final determination of the structure of the obtained bisspiropyran the data from X-ray crystallographic analysis were used (Fig. 1, Tables 1 and 2). The general appearance of the molecule of compound **3** is shown in Fig. 1.

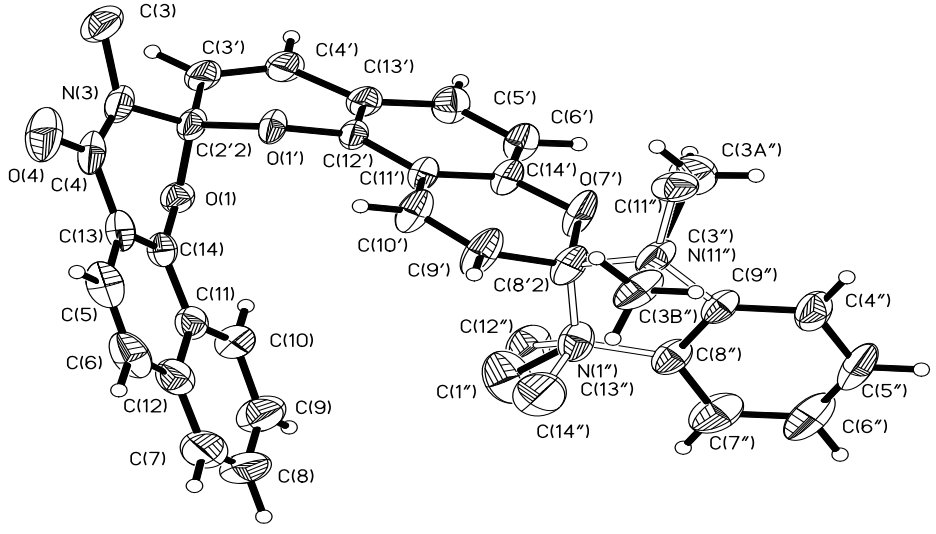

Fig. 1. The molecular structure of compound **3**.

The molecule of **3** is not planar. The angles between the plane of the central fragment of the molecule (C(2'2), O(1'), O(7'), C(3')–C(13'), C(8'2)) and the planes of the peripheral fragments (C(2'2), O(1), N(3), C(4), O(4), C(5)–C (13), and (C(8'2), N(1"), C(3")–C(9")) are 55.2 and 83.4° respectively, and the angle between the most peripheral fragments amounts to 100.8°.

Each fragment is nonplanar. The nonplanarity of the central fragment of the molecule is due to bending along the O(1')–C(3') and O(1')–C(4') lines by angles of 24.7 and 13.0° respectively. The peripheral fragments are nonplanar on account of bending along the O(1)–N(3), O(1)–C(4), and N(1")–C(3") lines by angles of 39.4, 8.0, and 31.1° respectively.

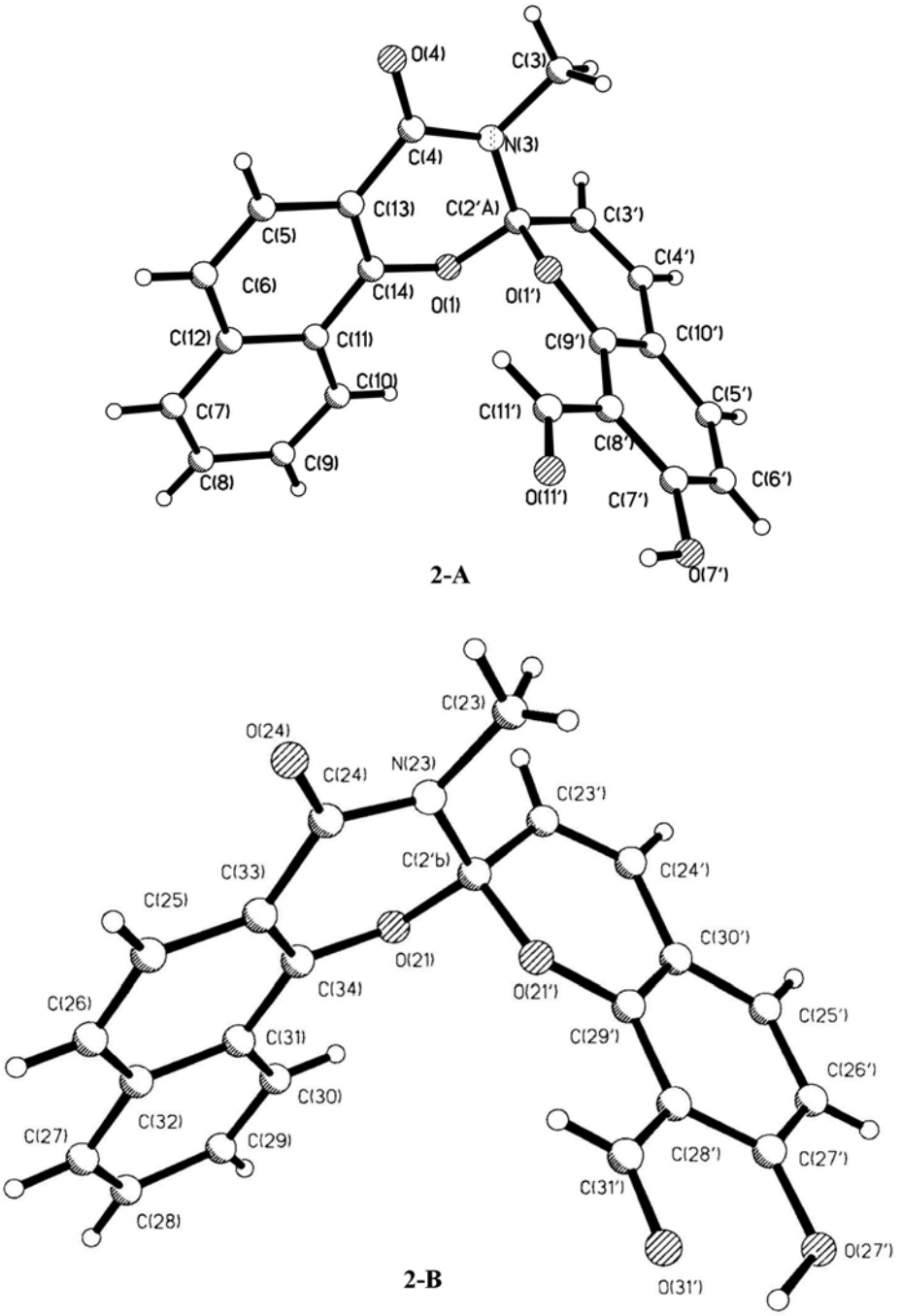

Fig. 2. The general appearance of the independent molecules **2-A** and **2-B**.

The distribution of the bond lengths in the spiro nodes C(2'2) and C(8'2) differs, and they are equal, respectively, to C(2'2)–N(3) = 1.421(3), C(2'2)–O(1) = 1.427(3), C(2'2)–C(3') = 1.492(4), C(2'2)–O(1') = 1.374(3), C(8'2)–N(1") = 1.471(4), C(8'2)–C(3") = 1.513(4), C(8'2)–O(7') = 1.472(3), C(8'2)–C(9') = 1.490(4) Å.

Earlier [1] the compound **2** shown in Fig. 2, which crystallizes in the form of two independent molecules **2-A** and **2-B**, was investigated.

The two independent molecules only differ from each other in the nature of the distribution of the bond lengths and bond angles. In both independent molecules of compound **2**, as in the molecule of the investigated compound **3**, the individual benzopyran and benzoxazinone fragments are nonplanar. The nonplanarity of the additionally annelated benzoxazine fragment in the independent molecule **2-A** is due to bending along the N(3)···O(1) and O(1)···C(4) lines by 37.3 and 4.7° respectively, while the nonplanarity of the benzopyran fragment is due to bending along the C(3')–O(1') and C(4')–O(1') lines by 20.3 and 8.1° respectively. The nonplanarity of the analogous fragments in the independent molecule **2-B** is due to bending along the N(23)···O(21) and O(21)···C(14) lines by 15.9 and 5.4° respectively. The values of the analogous bends in compound **3** are larger, and this is probably the reason for the significant discrepancy for the benzopyran fragments in the molecules of **2** and **3** with their juxtaposition on the plane of the benzoxazinone fragments (Fig. 3).

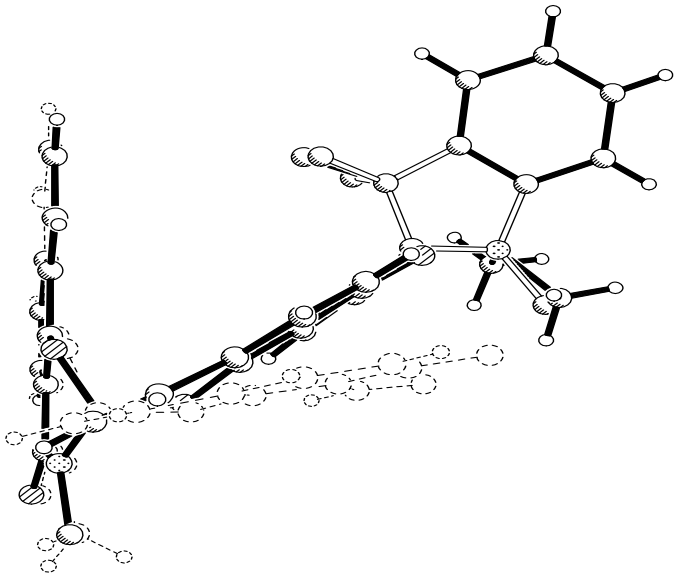

Fig. 3. Diagram of the molecule of compound **3** and of the previously investigated compound **2**, located on a common benzoxazinone fragment.

Like the analogous atoms in both independent molecules of compound **2** – the O(1), C(4), N(3), and O(4) atoms in **2-A** and O(21), C(24), N(23), and O(24) in **2-B** – the O(1), C(4), N(3), and O(4) atoms in compound **3** lie in the planes of the corresponding naphthalene fragments. Thus, the geometric structure of the C_{spiro}-node and the benzopyran fragment in the investigated compounds is similar to the structure of the previously investigated indoline and benzoxazine spiropyrans. In compound **3**, as also in compound **2**, the inclusion of the carbonyl group C(4)=O(2) in the benzoxazine fragment leads to a substantial change in the electronic and geometric picture of the structure of the N-node. The projection of the N(3) atom from the corresponding plane of the coordinating atoms C(2'2), C(4), and C(3) amounts to 0.171 Å, and the sum of the bonding angles at the N(3) atom is 355.7°. (The corresponding values for compound **3**, are 0.171 Å, 355.6° in **2-A** and 0.162 Å, 356.1° in **2-B** respectively). The length of the amide bond N(3)–C(4) = 1.353(4) Å in the bisspiropyran **3** is somewhat smaller than in the independent molecules **2-A** and **2-B** (1.375(4) and 1.375(4) Å respectively in **2-A** and **2-B**).

The photochromic characteristics of the bisspiropyran **3** were investigated. During irradiation of the bisspiropyran **3** with the unfiltered light in toluene three maxima appeared in the long-wave region of the absorption spectrum at 507, 422, and 613 nm (Fig. 4). The dark reaction of thermal decolorization of the photoinduced form leads to disappearance of the two absorption bands at 422 and 613 nm and retention of the maximum at 507 nm. However, disappearance of the absorption maximum at 507 nm in the UV spectrum was observed during irradiation with light of wavelength λ_{max} 435 nm (Fig. 5).

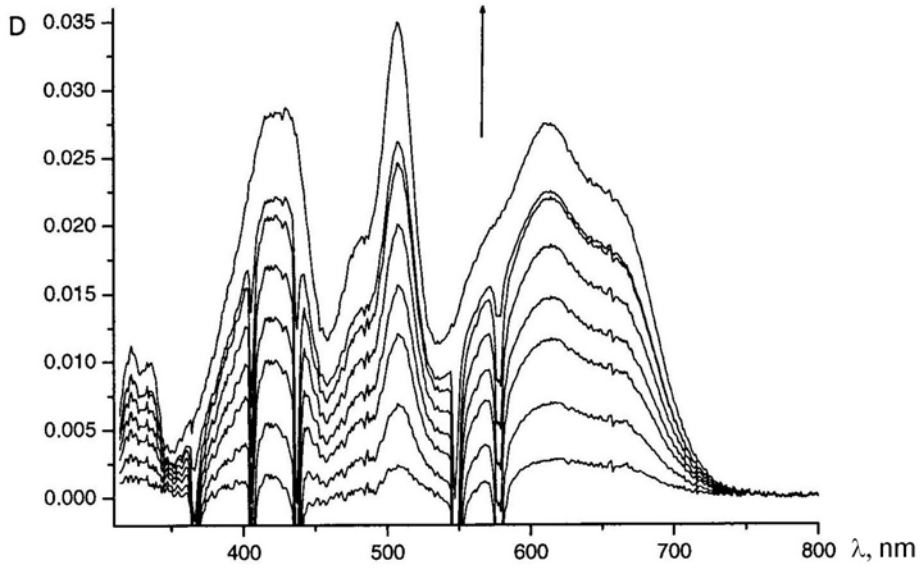

Fig. 4. The UV absorption spectrum of a solution of the bisspiropyran **3** in toluene before and after irradiation with unfiltered light under stationary conditions at 20°C. (The direction of change in the intensity of absorption with time is indicated by the arrow).

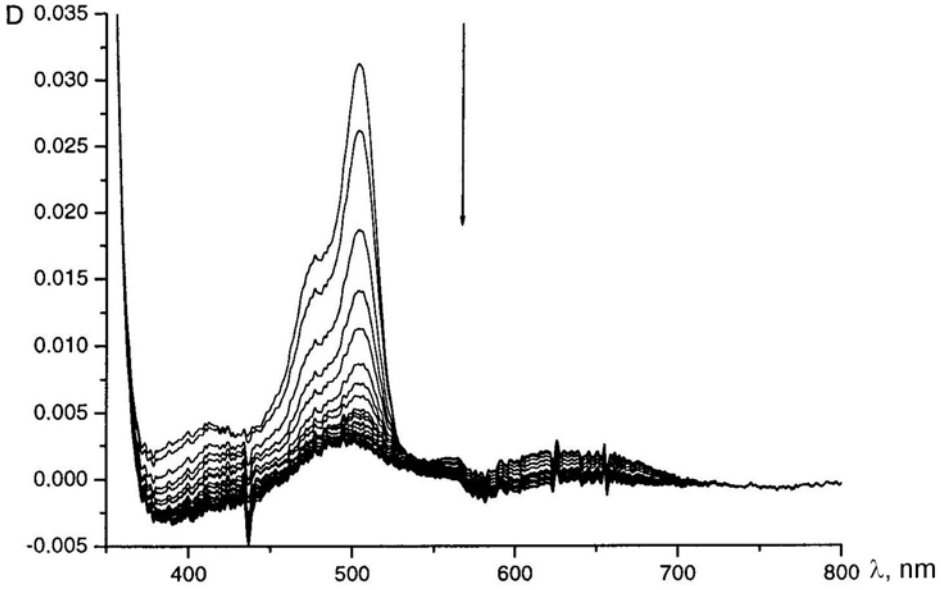

Fig. 5. The variation of the UV absorption spectrum of bisspiropyran **3** in toluene during irradiation with light with λ_{max} 436 nm at 20°C. (The arrow indicates the direction of variation of the intensity of absorption with time.)

The presence of several bands nonequivalent in behavior in the long-wave region of the absorption spectrum of the photoinduced form is atypical both for bissiropyrans and for compounds with single photochromic spirofragment. In order to interpret the observed changes in the spectral pattern by means of quantum-chemical calculations the nature of the electronic transitions corresponding to the maxima in the absorption spectra of the spiropyran **3** was investigated. By using density functional theory in terms of TD DFT (time-dependent density functional theory) with the hybrid Becke three-parameter Lee–Yang–Parr exchange–correlation functional (B3LYP) in the 6-31G** basis set it was possible to analyze the excitation energy of the respective singlet–singlet transitions.

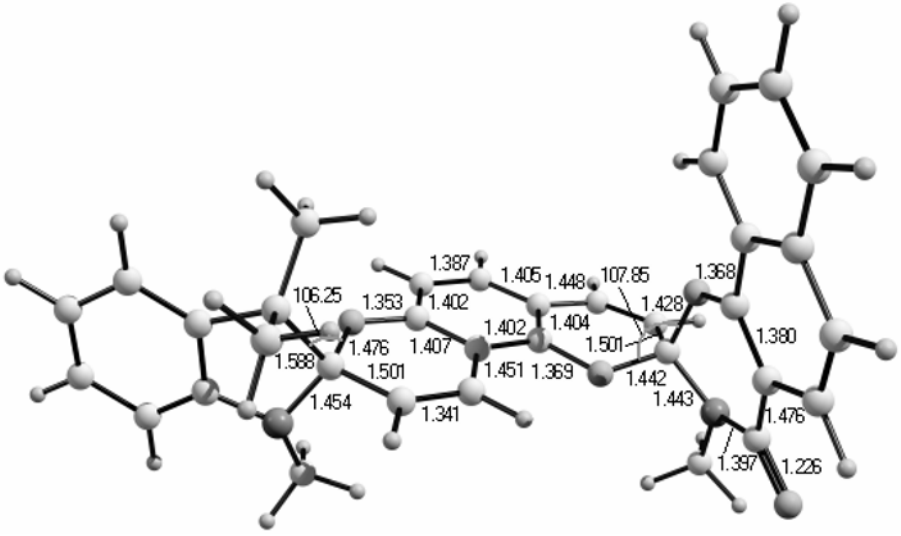

Fig. 6. The geometric parameters of the bisspiropyran **3** according to B3LYP/6-31G** results. The bond lengths are given in angstroms, the angles in degrees.

TABLE 1. The Principal Bond Lengths (*l*) in the Molecule of Bisspiropyran **3**

Bond	*l*, Å	Bond	*l*, Å
N(3)–C(4)	1.353(4)	N(3)–C(2'2)	1.421(3)
N(3)–C(3)	1.483(4)	C(4)–O(4)	1.232(3)
C(4)–C(13)	1.476(4)	C(5)–C(6)	1.335(5)
C(5)–C(13)	1.392(5)	C(6)–C(12)	1.425(5)
C(12)–C(7)	1.397(5)	C(12)–C(11)	1.421(4)
C(11)–C(10)	1.400(4)	C(11)–C(14)	1.415(4)
C(14)–C(13)	1.364(4)	C(14)–O(1)	1.366(3)
C(7)–C(8)	1.353(6)	C(8)–C(9)	1.411(5)
C(9)–C(10)	1.371(4)	O(1')–C(12')	1.374(3)
O(1')–C(2'2)	1.425(3)	O(1)–C(2'2)	1.427(3)
C(2'2)–C(3')	1.492(4)	C(3')–C(4')	1.314(4)
C(4')–C(13')	1.448(3)	C(5')–C(6')	1.370(4)
C(5')–C(13')	1.395(4)	C(6')–C(14')	1.376(4)
O(7')–C(14')	1.359(3)	O(7')–C(8'2)	1.472(3)
C(9')–C(10')	1.317(4)	C(9')–C(8'2)	1.490(4)
C(10')–C(11')	1.450(4)	C(11')–C(12')	1.386(3)
C(11')–C(14')	1.392(3)	C(12')–C(13')	1.389(3)
C(8'2)–N(1")	1.471(4)	C(8'2)–C(3")	1.513(4)
N(1")–C(8")	1.429(3)	N(1")–C(1")	1.461(8)
C(3")–C(9")	1.475(3)	C(3")–C(3A")	1.582(8)
C(3")–C(3B")	1.590(5)	C(4")–C(9")	1.367(4)
C(4")–C(5")	1.383(5)	C(5")–C(6")	1.346(6)
C(6")–C(7")	1.366(5)	C(7")–C(8")	1.384(4)
C(8")–C(9")	1.365(4)		

TABLE 2. The Valence Angles (ω) in the Molecule of Bisspiropyran **3**

Angle	ω, deg	Angle	ω, deg
C(4)–N(3)–C(2'2)	119.0(2)	C(4)–N(3)–C(3)	118.4(3)
C(2'2)–N(3)–C(3)	118.3(3)	O(4)–C(4)–N(3)	122.7(3)
O(4)–C(4)–C(13)	121.1(3)	N(3)–C(4)–C(13)	116.2(2)
C(6)–C(5)–C(13)	120.6(3)	C(5)–C(6)–C(12)	121.9(3)
C(7)–C(12)–C(11)	117.4(3)	C(7)–C(12)–C(6)	123.7(3)
C(11)–C(12)–C(6)	118.8(3)	C(10)–C(11)–C(14)	122.6(2)
C(10)–C(11)–C(12)	121.0(3)	C(14)–C(11)–C(12)	116.4(3)
C(13)–C(14)–O(1)	120.2(2)	C(13)–C(14)–C(11)	123.0(2)
O(1)–C(14)–C(11)	116.8(2)	C(14)–C(13)–C(5)	119.3(3)
C(14)–C(13)–C(4)	118.7(3)	C(5)–C(13)–C(4)	122.0(3)
C(8)–C(7)–C(12)	121.6(4)	C(7)–C(8)–C(9)	120.7(4)
C(10)–C(9)–C(8)	119.9(4)	C(9)–C(10)–C(11)	119.4(3)
C(12')–O(1')–C(2'2)	115.9(2)	C(14)–O(1)–C(2'2)	114.2(2)
N(3)–C(2'2)–O(1')	106.1(2)	N(3)–C(2'2)–O(1)	110.4(2)
O(1')–C(2'2)–O(1)	107.0(2)	N(3)–C(2'2)–C(3')	114.8(2)
O(1')–C(2'2)–C(3')	112.0(2)	O(1)–C(2'2)–C(3')	106.1(2)
C(4')–C(3')–C(2'2)	119.4(2)	C(3')–C(4')–C(13')	120.9(2)
C(6')–C(5')–C(13')	121.1(2)	C(5')–C(6')–C(14')	119.6(2)
C(14')–O(7')–C(8'2)	122.1(2)	C(10')–C(9')–C(8'2)	124.0(3)
C(9')–C(10')–C(11')	120.1(2)	C(12')–C(11')–C(14')	117.1(2)
C(12')–C(11')–C(10')	124.4(2)	C(14')–C(11')–C(10')	118.5(2)
O(1')–C(12')–C(11')	117.5(2)	O(1')–C(12')–C(13')	119.7(2)
C(11')–C(12')–C(13')	122.7(2)	C(12')–C(13')–C(5')	117.6(2)
C(12')–C(13')–C(4')	117.5(2)	C(5')–C(13')–C(4')	124.9(2)
O(7')–C(14')–C(6')	117.1(2)	O(7')–C(14')–C(11')	121.1(2)
C(6')–C(14')–C(11')	121.8(2)	N(1")–C(8'2)–O(7')	109.3(2)
N(1")–C(8'2)–C(9')	112.1(3)	O(7')–C(8'2)–C(9')	111.2(2)
N(1")–C(8'2)–C(3")	102.6(2)	O(7')–C(8'2)–C(3")	105.3(2)
C(9')–C(8'2)–C(3")	115.7(2)	C(8")–N(1")–C(1")	123.1(4)
C(8")–N(1")–C(8'2)	105.9(2)	C(1")–N(1")–C(8'2)	124.1(4)
C(9")–C(3")–C(8'2)	102.6(2)	C(9")–C(3")–C(3A")	111.3(4)
C(8'2)–C(3")–C(3A")	113.7(3)	C(9")–C(3")–C(3B")	108.1(2)
C(8'2)–C(3")–C(3B")	109.3(3)	C(3A")–C(3")–C(3B")	111.4(4)
C(9")–C(4")–C(5")	119.2(3)	C(6")–C(5")–C(4")	120.3(3)
C(5")–C(6")–C(7")	121.5(3)	C(6")–C(7")–C(8")	118.2(4)
C(9")–C(8")–C(7")	120.9(3)	C(9")–C(8")–N(1")	109.6(2)
C(7")–C(8")–N(1")	129.4(3)	C(8")–C(9")–C(4")	120.0(3)
C(8")–C(9")–C(3")	109.1(2)	C(4")–C(9")–C(3")	130.8(3)

The optimized geometry of the bisspiropyran **3** is shown in Fig. 6. The data from X-ray crystallographic analysis of this structure (Tables 1 and 2) agree fairly well with the calculated values.

According to theoretical estimates, the long-wave absorption band of the bisspiropyran should be observed in the region of 353 nm (energy of transition 3.626 eV), which corresponds with a fair degree of accuracy to the experimentally observed absorption in the region of 342 nm (3.515 eV).

As was established in a series of theoretical and experimental papers [7, 8], the thermodynamically most stable merocyanine form for a wide range of spiropyrans is the **TTC** (*trans-trans-cis* isomer). The following open forms of the bisspiropyrans were investigated: **TTC-TTC** (with two open pyran rings), **SP-TTC** (with a closed pyran fragment next to the indoline part and an open pyran fragment next to the naphthoxazine part), and **TTC-SP** (with an open pyran fragment next to the indoline part and a closed pyran fragment next to the naphthoxazine part) (Fig. 7).

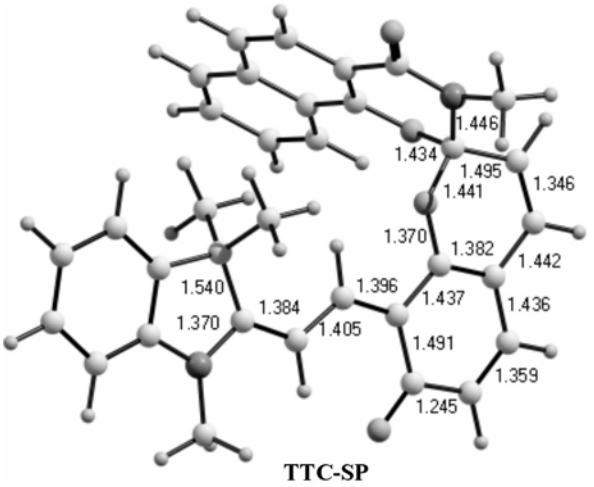

Fig. 7. The geometric parameters of the merocyanines **TTC-TTC**, **SP-TTC**, and **TTC-SP** according to data from B3LYP/6-31G** calculations.

The forms of the orbitals, the electronic transitions between which make contributions to the energy of the investigated excited states, are presented in Fig. 8 (for the **SP-TTC** isomer), Fig. 9 (for the **TTC-SP** isomer), and Fig. 10 (for the **TTC-TTC** isomer). The serial number and the type are shown next to the image of each orbital.

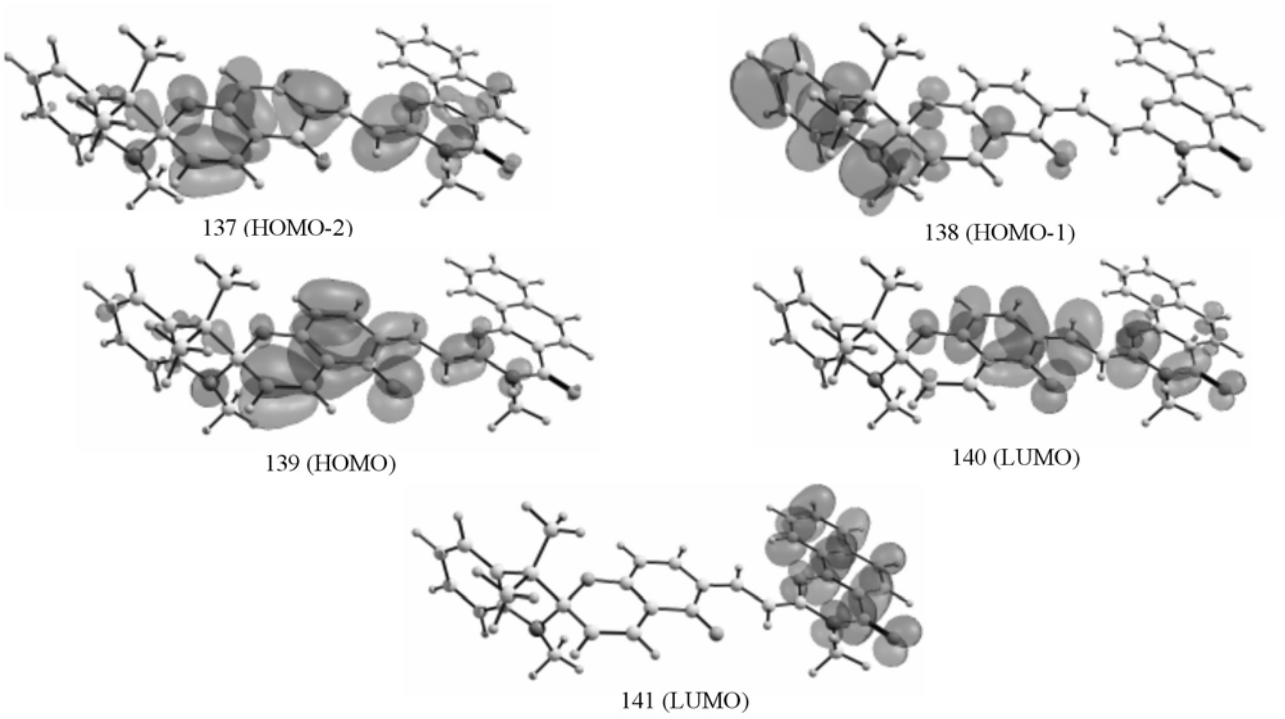

Fig. 8. The appearance of the molecular orbitals of the merocyanine **SP-TTC**, active in the electronic transitions during singlet–singlet excitation.

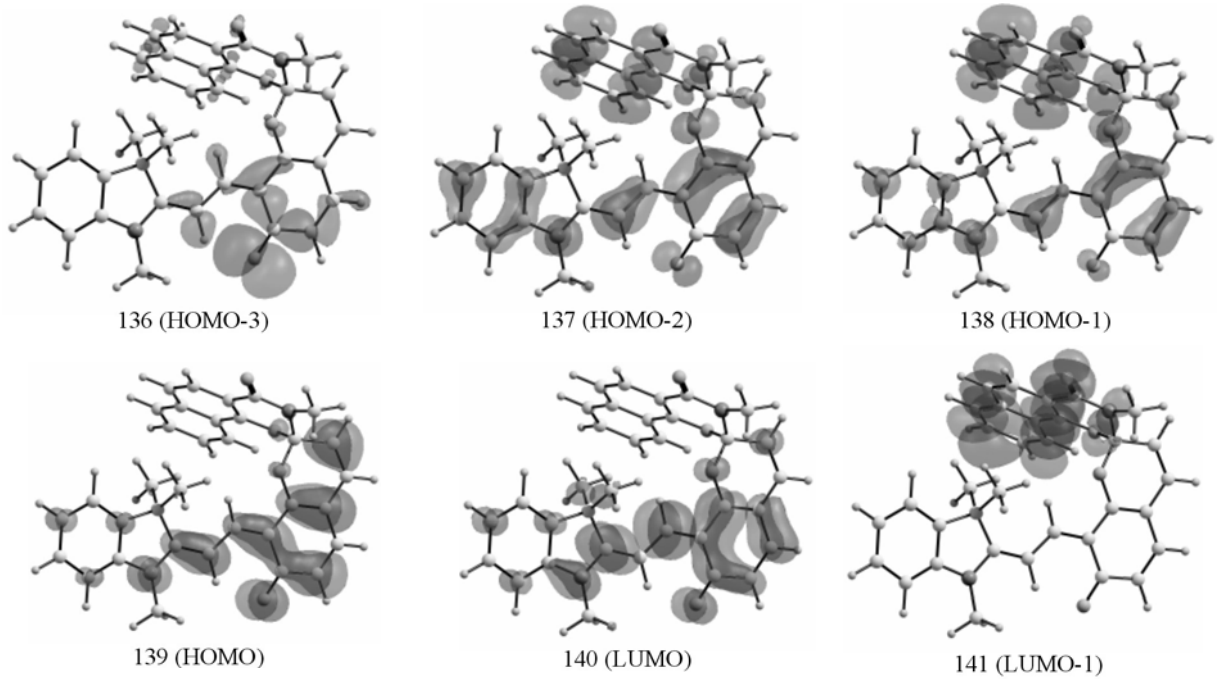

Fig. 9. The appearance of the molecular orbitals of merocyanine **TTC-SP**, active in the electronic transitions with singlet–singlet excitation.

The results of the calculations of the absorption spectra of the merocyanine isomers are given in Table 3.

As follows from the results of the calculations, the singlet excited states of the merocyanines **SP-TTC** and **TTC-SP** are largely determined by one orbital transition. For the first singlet excited states of these compounds this is the HOMO → LUMO π–π* transition arising from redistribution of the electron density in the open parts of each of the molecules. The S_0–S_2 transition in the **SP-TTC** structure is determined by the transfer of charge from the indoline to the chromene part of the molecule and corresponds to a low-intensity band in the absorption spectrum. For the **TTC-SP** structure this transition has *n*–π* character and corresponds to the transfer of charge from the carbonyl oxygen to the π*-orbital of the open indoline part of the molecule. The third excited singlet for the **SP-TCC** and **TTC-SP** merocyanines has the nature of charge transfer from the pyran to the naphthoxazine fragment and also has a low intensity for the transition.

The absorption bands of the completely open bisspiropyran are more complicated in nature. This is due to the fact that comparable contributions to the energy of the excited singlet states lead at once to several electronic transitions.

Thus, for the first singlet these are the two transitions involving transfer of charge from the indoline fragment and part of the pyran fragment to another open fragment and back and two π–π* transitions in the indoline and the open pyran part of the molecule. A band for charge transfer from the pyran to the naphthoxazine fragment corresponds the S_0–S_2 transition. The three π–π* electronic transitions (HOMO → LUMO+2, HOMO−1 → LUMO, HOMO−1 → LUMO+1) and two charge transfer transitions (HOMO → LUMO and HOMO−1 → LUMO+2) make contributions to the energy of the third singlet. This transition has significantly higher intensity than the first two, and it must correspond to the observed long-wave maximum in the absorption spectrum.

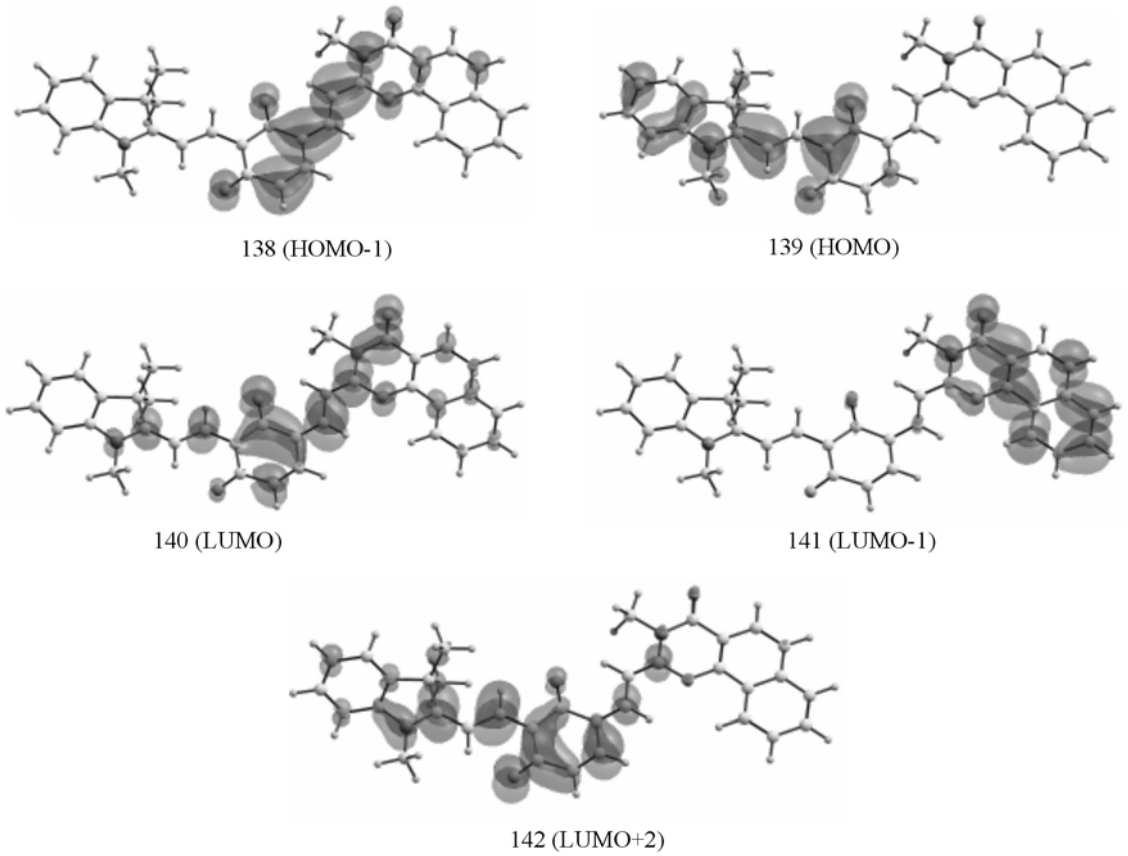

Fig. 10. The appearance of the molecular orbitals of merocyanine **TTC-TTC**, active in the electronic transitions with singlet–singlet excitation.

TABLE 3. The TD B3LYP/6-31G** Calculated (ΔE_{calc}) and Corrected (ΔE_{theor}) Excitation Energies and the Oscillator Forces (f) of the Singlet–Singlet Transitions in the Merocyanine Isomers of Bisspiropyran **3**

Structure	Transition	Nature of transition		ΔE_{calc}, eV	f	ΔE_{theor}, eV	ΔE_{ex}^{exp}, eV
		Transition orbitals	Contribution				
TTC-TTC	S_0–S_1	138 – >140	–0.1575	2.6797	0.0098	2.225434	
	CT	138 – >142	–0.33992				
		139 – >140	0.5072				
		139 – >142	–0.28183				
	S_0–S_2	138 – >140	–0.21647	2.7598	0.0109	2.301849	
	CT	138 – >141	0.65708				
	S_0–S_3	138 – >140	0.40632	2.8463	0.2681	2.38437	2.455446
	π–π^*	138 – >141	0.18831				
		138 – >142	0.36119				
		139 – >140	0.22031				
		139 – >142	–0.28754				
SP-TTC	S_0–S_1	137 – >140	–0.17102	2.3254	0.1228	1.887432	1.89313
	π–π^*	138 – >140	0.12657				
		139 – >140	0.61981				
	S_0–S_2	138 – >140	0.68768	2.4597	0.0564	2.015554	
	CT	139 – >140	–0.13174				
	S_0–S_1	137 – >141	0.12647	2.6144	0.0006	2.163138	
	CT	139 – >141	0.68899				
TTC-SP	S_0–S_1	137 – >140	0.10387	2.3612	0.3093	1.921585	
	π–π^*	138 – >140	–0.10147				
		139 – >140	0.60493				
	S_0–S_2	136 – >140	0.64795	2.6128	0.0005	2.161611	
	n–π^*	137 – >140	–0.196				
		138 – >140	–0.11399				
	S_0–S_3	137 – >140	0.11741	3.037	0.0119	2.566298	
	CT	138 – >140	0.31913				
		139 – >141	0.60801				

It is known that TD DFT theory gives systematically high values for the excitation energies for the merocyanine isomers of spirocyclic compounds [9]. Therefore the method proposed in [10] was used for correlation of the calculated energies of the transitions. New values for the energies of the transitions were calculated from the obtained linear relationship between the experimentally observed and theoretically predicted excitation energies of the type: $\Delta E_{theor} = -0.311 + 0.954*\Delta E_{calc}$.

It should be noted that according to the data from the calculations the long-wave absorption band of the fully open bisspiropyran **TTC-TTC** must lie in a region of shorter wavelengths than the absorption bands of the merocyanines **SP-TTC** and **TTC-SP**. This can be explained by the fact that the main contribution to the excitation energy of the **TTC-TTC** molecule, corresponding to the strongest absorption band, comes from the electronic transitions between the nonadjacent molecular orbitals, whereas the long-wave absorption for the **SP-TTC** and **TTC-SP** isomers is due to the HOMO → LUMO transitions.

As follows from the data presented in Table 3, the observed absorption band in the region of 507 nm (2.455 eV) must correspond to the absorption of the fully open bisspiropyran whereas the absorption in the region of 655 nm (1.893 eV) is most likely due to singlet–singlet transitions in the merocyanines **SP-TTC** or **TTC-SP**.

Thus, the data from the quantum-chemical calculations show that irradiation of the bisspiropyran **3** with unfiltered light leads to opening of both pyran rings. This result is of fundamental significance since it is the

first example of simultaneous opening of both 2H-pyran rings in the series of spiropyrans and shows that this is only possible in the case of unsymmetrical bisspiropyrans, whereas opening of only one 2H-chromene ring was observed in all previously studied symmetrical compounds of this type.

EXPERIMENTAL

The electronic absorption spectra were recorded on an Agilent 8453 spectrophotometer. The irradiation source was a DRSh-250 mercury lamp with the standard set of filters.

The unit cell parameters of a crystal of compound **3** and a three-dimensional set of reflection intensities were obtained on a Kuma Diffraction KM-4 diffractometer (MoKα radiation, graphite monochromator) with a colorless single crystal measuring 0.40×0.40×0.40 mm. Basic crystallographic data of compound **3**: $C_{34}H_{20}N_2O_4$, crystallizes in the monoclinic system with a = 14.783(2), b = 11.269(2), c = 16.759(3) Å, β = 100.58°(2), V = 2744.4(8) Å^3, M_r = 520.52, space group $P2(1)/c$, Z = 4, d_{calc} = 1.260 g/cm^3. The intensities of 4960 reflections were measured in an independent part of reciprocal space ($\theta \leq 24.97°$) by the ω/2θ scanning method. After exclusion of the systematically extinguished and equivalent reflections the working set of measured reflections amounted to 4763, of which 3290 were with $I > 2\sigma(I)$. The structure was interpreted by the direct method and refined by full matrix least squares analysis of F^2 using the SHELX-97 software in the approximation of anisotropic thermal vibrations for the non-hydrogen atoms. All the hydrogen atoms in the structure were found by difference syntheses and were refined by the "rider" model [11]. In the last cycle of full-matrix refinement the absolute shifts of all 384 variable parameters of the structure of **3** were less than 0.001σ. The final parameters of the refinement were: R_1 = 0.061, wR_2 = 0.16 for 3290 observable reflections with $I \geq 2\sigma(I)$; R_1 = 0.085, wR_2 = 0.18 for all 4763 measured reflections, $GOOF$ = 1.046. When the refinement was complete the maximum and minimum values of the electron density differences amounted to 0.283 and -0.207 eÅ^{-3}. The final distances and angles in the molecule are given in Table 1.

The work was carried out with financial support from State contract No. P-1473, Grant from the President of the Russian Federation NSh-363.2008.3, and Grant RNP 2.2.1.1/2348.

REFERENCES

1. E. L. Mukhanov, Yu. S. Alekseenko, B. S. Lukyanov, V. I. Minkin, S. O. Bezuglyi, A. N. Utenyshev, V. V. Tkachev, and S. M. Aldoshin, *Khim. Geterotsikl. Soedin.*, 273 (2009). [*Chem. Heterocycl. Comp.*, **45**, 219 (2009)].
2. B. S. Lukyanov and M. B. Lukyanova, 323 (2005). [*Chem. Heterocycl. Comp.*, **41**, 281 (2005)].
3. V. I. Minkin, *Chem. Rev.*, **104**, 2751 (2004).
4. D. H. Duerr and H. Bouas-Laurent, *Photochromism. Molecules and System*, Elsevier, Amsterdam (1990), p. 1068.
5. V. Weiss, A. A. Friesem, and V. A. Krongauz, *J. Appl. Phys.*, **74**, 4248 (1993).
6. E. L. Mukhanov, Yu. S. Alekseenko, B. S. Lukyanov, Yu. I. Ryabukhin, O. N. Ryashchin, and M. B. Lukyanova, *Khim. Geterotsikl. Soedin.*, 129 (2007). [*Chem. Heterocycl. Comp.*, **43**, 111 (2007)].
7. Y. Futami, M. Chin, S. Kudoh, M. Takayanagi, and M. Nakata, *Chem. Phys. Lett.*, **370**, 460 (2003).
8. G. Cottone, R. Noto, G. La Manna, and S. L. Fornili, *Chem. Phys. Lett.*, **319**, 51 (2000).
9. A. Dreuw, J. L. Weisman, and M. Head-Gordon, *J. Chem. Phys.*, **119**, 2943 (2003).
10. M. Guillaume, B. Champagne, and F. Zutterman, *J. Phys. Chem. A*, **110**, 13007 (2006).
11. G. M. Sheldrick, *SHELXL-97, Program for Refinement of Crystal Structures*, Univ. Göttingen (Germany) (1997).